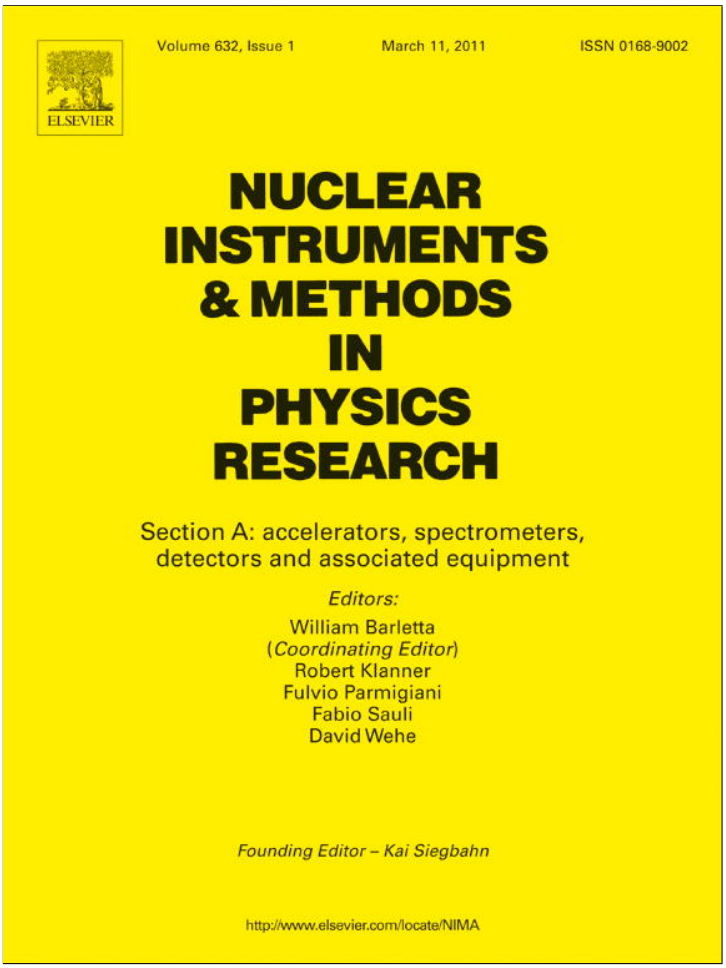

Nuclear Instruments and Methods in Physics Research A 632 (2011) 147–151

Contents lists available at ScienceDirect

Nuclear Instruments and Methods in Physics Research A

journal homepage: www.elsevier.com/locate/nima

A complete dosimetric characterization of two ^{90}Sr–^{90}Y dermatologic applicators

T.S. Coelho [a], M.A.R. Fernandes [b], H. Yoriyaz [a,*], P.L. Antonio [a]

[a] Instituto de Pesquisas Energéticas e Nucleares, IPEN/CNEN, São Paulo, Brazil
[b] Faculdade de Medicina de Botucatu, UNESP, Departamento de Dermatologia e Radioterapia, São Paulo, Brazil

ARTICLE INFO

Article history:
Received 22 November 2010
Received in revised form
17 December 2010
Accepted 18 December 2010
Available online 1 January 2011

Keywords:
Betatherapy
Monte Carlo method
Keloids
Pterygium
Dosimetry

ABSTRACT

A complete dosimetric characterization of two Amershan ^{90}Sr–^{90}Y dermatologic applicators is described in this present work. The dosimetric parameters analyzed are: percentage depth dose curve, radial dose distribution, non-uniformity and asymmetry. Both applicators are planar–circular having 22.57 and 9.0 mm diameters. In the range where the percentage depth dose goes from 100% down to 20%, the measured percentage depth dose and that obtained by the Monte Carlo simulation have shown maximum discrepancy of 5.3% for both applicators. The radial dose distribution has been measured at several depths using a *GafChromic*® EBT QD+ films and it was also calculated by simulation. The discrepancies found did not exceed 5.9% up to the depth of 1.8 mm, where the percentage depth dose drops to 40% of the maximum. The maximum non-uniformity and asymmetry are 1.7% and 5.3% for the first applicator and 22.7% and 25.9% for the second applicator, respectively. Both applicators meet the specification for the maximum non-uniformity established by the adopted protocol, whose limit is 30%. As for the asymmetry the limit is 20% and the second applicator exceeded it in about 5.9%.

1. Introduction

Skin lesion, like keloid, is a pathology that is characterized by an excessive production of fibrous tissue as a consequence of some coetaneous trauma or surgical excision [1]. It is pronounced in children and adolescents with more incidences in women than in men and in people with dark skin and eastern descendants [2,3]. For patients, keloids are not only a matter of cosmetic question, but depending of the body's region, it can cause burning sensation, itching, tingling or pain. New formed keloids, rich in fibroblasts, are highly radiosensitive, so that, the exposure to radiation can inhibit the proliferation of fibrous tissue [4].

Pterygium is a benign disease originated from a newly formed fibrovascular conjunctival bulb. This lesion has a triangular shape, which can occur in temporal or nasal limbus. [5]. The most common treatment is the surgical excision; however, recurrence rate around 20–40% is reported. Among the various techniques used after surgery to prevent recurrence of pterygium, radiotherapy with beta rays has shown better results, reducing this rate to 20% or less [6,7].

Due to its long half-life (28.5 years), ^{90}Sr–^{90}Y betatherapy applicators are still in use worldwide especially for very superficial skin lesions like keloids and pterigium. However, most of these applicators dot not follow a regular dosimetric characterization due to the fact that this procedure involves an exceedingly laborious task to be done at clinical centers. These aspects added to the non existence of an international agreement on the standard procedure rise the necessity to achieve a methodology to completely characterize those applicators.

In this work a complete dosimetric analysis has been performed for two Amershan betatherapy ^{90}Sr–^{90}Y circular–planar applicators. Percentage depth dose curves and radial dose distributions at several depths have been measured using ionization chamber and radiochromic films. The non-uniformity and asymmetry parameters have also been determined using the methodology that is described in Section 3. The experimental values were compared to those calculated by the Monte Carlo simulation using the MCNP5 code [8].

2. Material and methods

2.1. ^{90}Sr–^{90}Y applicators

The applicators are typically composed of metal plates in which the ^{90}Sr–^{90}Y is deposited on the surface. These plates are flat with dimensions of 22.57 and 9.0 mm diameter and denominated here as applicators 1 and 2, respectively. The face of the plate placed in contact with the skin is covered by polyethylene with a thickness of approximately 1.0 mm in order to shield the

* Corresponding author.
E-mail address: hyoriyaz@ipen.br (H. Yoriyaz).

0168-9002/$ - see front matter © 2010 Elsevier B.V. All rights reserved.
doi:10.1016/j.nima.2010.12.179

low-energy electrons that are generated during the decay of ^{90}Sr. These applicators have a primary barrier composed of a low atomic number material such as plastic with a thickness of about 10.0 mm for protection during application handling.

2.2. Radiochromic films

The advantage of radiographic films over other dosimeters is the high spatial resolution. Presently, a new type of film has been used in radiotherapy services, which is the radiochromic film. This film needs no darkroom during handling, it is self-revealing and can be used for dosimetry in regions with high dose gradient and has higher spatial resolution than radiographic films. In the present work, the *GafChromic*® EBT DR+ film manufactured by the International Specialty Products [9] has been used. This film is composed of two layers of active components that are separated by the surface layer and coated with polyester and is designed for a range of dose from 0.01 to 8 Gy.

2.3. Extrapolation ion chamber

^{90}Sr–^{90}Y applicators produce a very high dose gradient in a very short distance requiring measurements in small volumes. The recommended ion chambers for this condition are the extrapolation chambers. This type of detector allows the variation of its sensitive volume by changing the distance between the electrodes of the chamber. The detector used in the present work was a parallel plate mini-extrapolation chamber, developed at the Calibration Laboratory of IPEN, connected to a PTW electrometer model UNIDOS 10001.

2.4. Monte Carlo code MCNP5

Simulations of radiation transport for energy deposition calculation have been accomplished by the Monte Carlo code MCNP5 [8]. The entire simulation problem is described through an input archive where all informations like geometric dimensions, source information and material components are provided. Other input parameters are the total number of particle histories to be simulated, energy cut-off, cross-section libraries and variance reduction technique options. Specifically for electron transport, MCNP5 is classified as class I, therefore, it is restricted to use the condensed history method where the path of the particles is divided into so-called energy steps. In each energy step, the mean effect of a large number of individual interactions is considered. In this method, all cross-sections are calculated on a fixed energy grid where the energy steps are predefined in the code by the logarithmic decrease of energy of about 8.3%. Sampling of energy loss obeys the Landau distribution with the Blunck–Leisegang correction and enlargement factor by Seltzer for low path lengths. The sampling of the angular distribution is given according to the theory of Goudsmit–Saunderson [10].

The photon transport is simulated in great detail, interaction by interaction. Secondary particles are generated by the differential cross-sections (DCS) of Bhabha and Møller [11] along the pathway and stored in an array to be transported afterwards. The model considers the photoelectric effect, Compton and Rayleigh scattering and pair production.

3. Dosimetric parameters

3.1. Percentage depth dose (PDD) and radial dose distribution (RDD)

Dose measurements were done in a phantom composed by a set of 0.6 mm thickness polyethylene plates to simulate the skin. The PDD curve represents the percentage ratio of the dose at a given depth (D_p) in the phantom to the maximum dose (D_{max}) in the central axial axis. The RDD is defined by the percentage ratio of doses at given distances from the central axis relative to the maximum dose at a certain depth in the phantom.

3.2. Non-uniformity and asymmetry

Non-uniformity (UF) is defined as the maximum allowable percentage change in dose within 80% of the width at half maximum of the field profile (R_{50}) in a plane transverse to the beam axis. The mathematical definition is given by Eq. (1) below [12]:

$$U_F = \max\left(D_{min}-D_{r=0}\right|,\left|D_{max}-D_{r=0}\right|)/D_{r=0}\times 100 \quad (1)$$

where D_{max} and D_{min} are the maximum and minimum dose, respectively, in the range from $r=0$ to $r=0.8R_{50}$ and $D_{r=0}$ is the dose $D(r, z)$ determined at the central axis of the radiation source ($r=0$) and at a depth of $z=2$ mm.

The asymmetry (U_{assym}) is the variation of the dose calculated on a circle with radius r. The maximum of this variation in the range from $r=0$ to $r=0.8R_{50}$ determines the value of the asymmetry. This parameter is calculated by Eq. (2) below:

$$U_{assym} = \max\left(\{D_{max}(r)-D_{min}(r)\}/D_{avg}(r)\right)\times 100 \quad (2)$$

where D_{avg} is the average absorbed dose in a set of dose values ranging from $r=0$ to $r=0.8R_{50}$.

In the present work these parameters have been determined by an array of pixels taken from the scanned images of the irradiated radiochromic films. In this case, the non-uniformity and asymmetry of the source can be defined through the determination of the field center and seeking the maximum change in a surrounding area and extended from the center of the field up to 50% isodose curve. The field center is defined as the center of the 50% isodose curve, which is the center of the area in which the relative dose measured at a depth of 2.0 mm is 50% or more of the maximum dose in this plane [12,13].

Mathematically, one can calculate the field center from an array of pixels in a cartesian coordinate system. The method consist in finding the coordinates of the 50% isodose curve center, (x_c, y_c) and the coordinates of the chosen points $x50_k$ and $y50_k$, which afterwards will be used for the determination of the average radius, R_{50}. The coordinates of the field center, (x_c, y_c), are given by

$$x_c = \left(\frac{1}{n}\right)\sum_{i=1}^{n}\frac{x50_i^- + x50_i^+}{2} \quad (3)$$

$$y_c = \left(\frac{1}{n}\right)\sum_{j=1}^{n}\frac{y50_j^- + y50_j^+}{2} \quad (4)$$

where $x50_i^+$, $x50_i^-$, $y50_j^+$ and $y50_j^-$ are the positions in x and y, respectively, delimiting the 50% isodose curve and n is determined by the amount of points chosen.

The positions mentioned above are determined by linear interpolation of the ith row or jth column. The position $x50_i^-$ indicates the position of the pixel on the left side of the source in the 50% isodose curve and $x50_i^+$ indicates the position of the pixel on the same line as $x50_i^-$, but situated at the right side of the source in the 50% isodose curve. Once these two points are obtained, an interpolation of the positions of these two pixels is made to find the x position of the central pixel of the source, x_c. The same procedure is used for positions $y50_j^-$ and $y50_j^+$, where $y50_j^-$ represents the position of the pixel below the central source in the 50% isodose curve and $y50_j^+$ indicates the position of the pixel in the same column of $y50_j^-$ and above the center of the source in the 50% isodose curve. The interpolation of these two positions gives the y position of the central pixel of the source, y_c.

The positive sign (+) of $x50_i$ and $y50_i$ values indicates, respectively, the right and above positions relative to the center of the source, and

the negative (−) sign indicates, respectively, the left and below positions related to the center of the source. Fig. 1 illustrates the 50% isodose curve obtained from the scanned image and the x and y positions for the determination of the field center. The square symbols indicate the location of the coordinates $x50_i^{\pm}$ and the spheres indicate the location of the coordinates $y50_i^{\pm}$. The value n is the number of rows or columns containing values of the dose greater than 50% of the maximum dose. This value is determined by the amount of points chosen in the line.

Once the coordinates of the source center, (x_c, y_c), are found, the average radius, R_{50}, which is defined as the average radius of the 50% isodose curve, can be calculated by [12]

$$R_{50} = \left(\frac{1}{n}\right) \sum_{k=1}^{n} \sqrt{(x_c - x50_k)^2 + (y_c - y50_k)^2} \quad (5)$$

4. Results and discussion

4.1. Percentage depth dose

Percentage depth dose (PDD) has been measured utilizing a mini-extrapolation chamber and calculated by the MCNP5 Monte Carlo simulation. The behavior of these sources reveals a great ionization power in a short tissue range, which makes the dose measurements and the precise dose calculation in small target volumes challenging tasks.

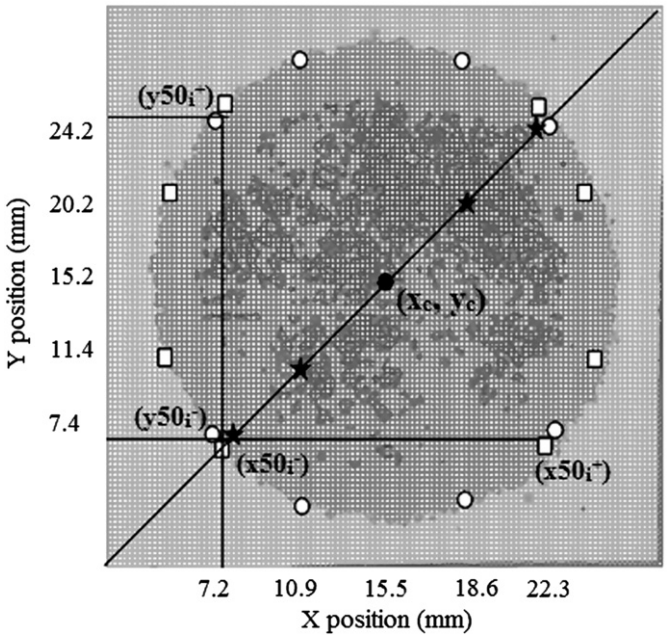

Fig. 1. 50% isodose curve obtained from scanned film image for field center determination, (x_c, y_c).

The maximum radiation dose occurs at the tissue surface and decreases rapidly down to 30% of the maximum dose at 3.0 mm of depth. The maximum discrepancy found between measured and calculated values is less than 5.3% for both applicators in the range from the surface to 3.0 mm depth. The experimental and simulated uncertainties were 2.0% and 0.3%, respectively. Monte Carlo simulations were done with 10 million particle histories. Fig. 2 shows the calculated and measured results obtained for both applicators.

The ICRU report 72 [13] proposes an adjusted curve based on several applicators with an active diameter of 8.6 mm. Measured and calculated values served to build an empirical function to represent an average curve to be used as a reference for similar applicators. Following this procedure, specific functions for the applicators utilized here have been built based on calculated PDD curves. The empirical expression used was:

$$\frac{D(z, r_0 = 0)}{D(z_0 = 0, r_0 = 0)} = \exp(a + bz + cz^2 + dz^3 + ez^4 + fz^5) \quad (6)$$

where the coefficients a, b, c, d, e and f are to be determined by curve adjustment, $r_0 = 0$ refers to the central axis, z is the depth in the phantom and $z_0 = 0$ refers to the surface of the phantom where the maximum dose occurs.

Table 1 presents the coefficient values obtained from the exponential curve adjustment. Once the coefficients have been determined, the PDD curves for the applicators have been plotted and compared to that provided by the ICRU report 72. As one can observe from Fig. 2b, for applicator 2, whose diameter is very similar, the adjusted exponential curve agrees well with the ICRU data with a maximum discrepancy less than 3.0%, indicating that the simulation data reproduced satisfactorily well the PDD data. As for the applicator 1, its diameter is more than twice that of the applicator 2 and of the reference (ICRU) applicator. This difference introduces discrepancies of the order of 7.5–13%, showing the influence of the applicator's diameter in the dose profile. Another contribution for the discrepancies found here, in general, can be attributed to uncertainties in the geometry dimensions of the applicator specially, the uncertainty on the thickness of the polyethylene material that covers the face of the applicator that is in contact with the phantom surface. This is particularly important for short range beta particles that cause high dose gradient as observed here and where small differences in the material thickness can provoke considerable changes in the dose profile. Besides this fact, the ICRU data uncertainties are of the order of 6.0% or more.

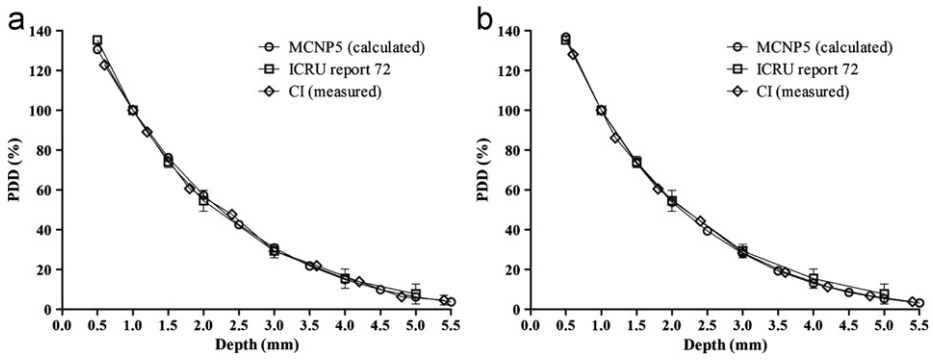

Fig. 2. Comparison of measured and calculated PDD taken from the ICRU report 72 for (a) applicator 1 and (b) applicator 2.

4.2. Radial dose distribution

Radial dose distributions have been measured using the *GafChromic*® EBT QD+ films and also calculated by the Monte Carlo simulation. The film dosimetric characterization process was performed by obtaining the sensitometric curve and achieving the best optical density range and linearity region. Knowing the applicators dose rate given by the manufacturer the film characterization procedure was made exposing it to several known dose values ranging from 0.33 to 4.93 Gy.

The films were exposed at two depths: 0.6 and 1.8 mm. Optical densities were measured using a PTW DensiX densitometer and then correlated to the exposed doses and to the average gray level of a group of pixels, taken from the film scanned images read by the auxiliary of the ImageJ software [14]. In this aspect, each point in the measured radial dose curve corresponds to a mean gray level value belonging to a group of pixels. The standard deviation of the mean varied from 0.5% to 8.0% from the center to the border of the image.

Following this procedure the radial dose distribution has been plotted considering the average gray level of a group of pixels in a radial direction, starting from the central axis position that was assumed as the geometric center of the scanned images. Calculated radial dose distributions also have been obtained through the Monte Carlo simulation with 20 million particles histories to achieve maximum uncertainty of 1.14%. The comparisons of these results with experimental data are shown in Fig. 3. For both applicators, the maximum relative dose differences were 5.9% and 5.7% at 0.6 and 1.8 mm depth, respectively. These differences are completely reasonable and within the statistical uncertainties considering the standard deviation of the calculated and measured mean values.

The agreement between Monte Carlo simulation results in radial dose distribution determination and those obtained through radiochromic film measurements found here, gave confidence to proceed with the determination of non-uniformity and asymmetry parameters, which is described in the next section.

Table 1
Coefficients of the PDD exponential functions for applicators 1 and 2 based on calculated values.

Coefficient	ICRU report 72	Applicator 1	Applicator 2
a	0.5608	0.5542	0.6438
b	−0.4913	−0.5931	−0.7184
c	−0.09887	0.06049	0.10899
d	0.03619	−0.0269	−0.04298
e	−0.00723	0.00358	0.00633
f	0.0004487	−0.0002408	−0.0004125

4.3. Non-uniformity and asymmetry

Non-uniformity and asymmetry have been determined according to the methodology described in the previous section that was based on the Netherlands Commission on Radiation Dosimetry (NCS) protocol [12]. After the determination of the field center coordinates according to Eqs. (3) and (4), the region of interest (ROI), which corresponds to the isodose area of 50%, delimited by R_{50} and $0.8R_{50}$ has been defined. The shaded areas in Fig. 4 represent the ROI in the radial dose distributions at 1.8 mm depth obtained from experimental measurement for both applicators. The calculation of non-uniformity and asymmetry was made identifying D_{min}, D_{max}, $D_{r=0}$, and D_{avg} in the ROI. For applicator 1, the non-uniformity was 1.7% and the asymmetry was 5.3%. For applicator 2, the value of non-uniformity was 22.7% and the value of the asymmetry was 25.9%.

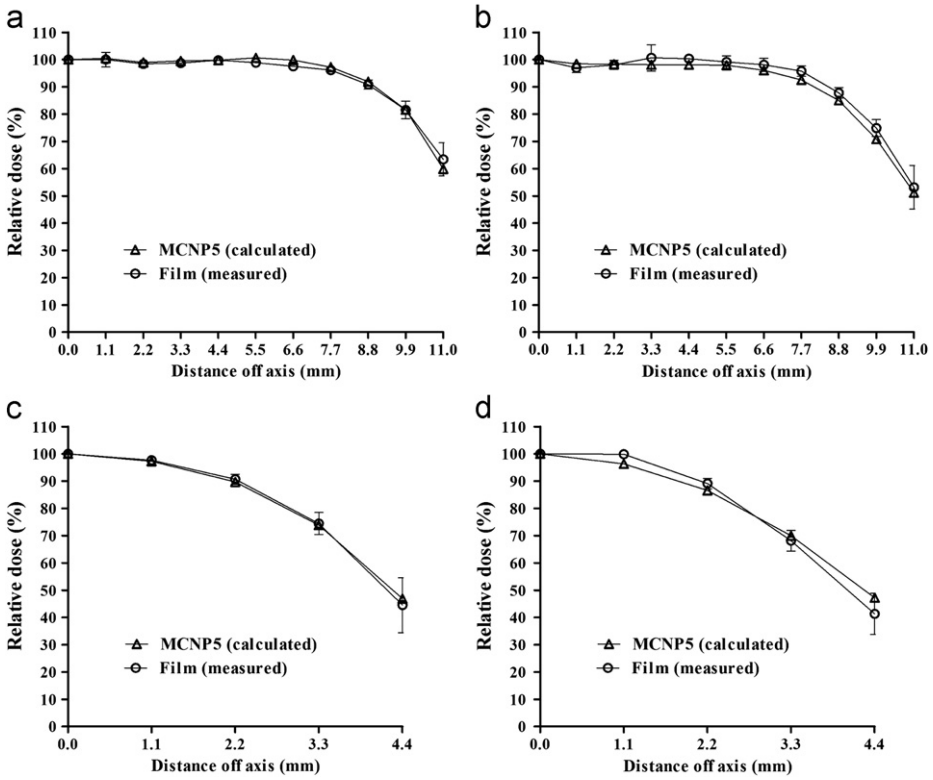

Fig. 3. Radial dose distributions at 0.6 and 1.8 mm depth for: Applicator 1, (a and b) and applicator 2 (c and d).

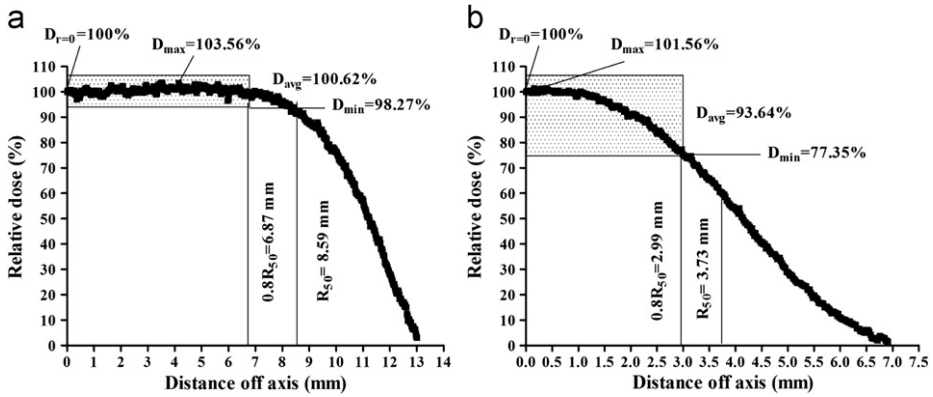

Fig. 4. Region of interest of the radial dose distribution for non-uniformity and asymmetry calculations defined in the radial dose distribution: (a) applicator 1 and (b) applicator 2.

It can be observed that the values of non-uniformity and asymmetry obtained for the applicator 1 are within the recommended limits, where according to NCS protocol, the non-uniformity must be less than 30% and the asymmetry less than 20%. For applicator 2, the non-uniformity is within the limit, but the asymmetry value was 5.9% beyond the limit established by the criteria. However, considering the fact that the experimental uncertainty in the radial dose distribution is about 8.0% and it propagates to the associated asymmetry error, this exceeding limit of 5.9% in the asymmetry value could be considered acceptable.

5. Conclusion

Comparison of calculated and measured dosimetric parameters and also with those provided by the ICRU report 72 showed good agreement among them, demonstrating the suitability of the calculation methodology adopted in the present work. The maximum dose discrepancy between measured and calculated PDD values were within 5.3% and most of it due to the complexity caused by the applicators size and radiation nature, requiring special concerns and the necessity of high geometric resolution measurement tools. This is because the dose gradient is very high in a very short range requiring measurements in small volumes. In the present work these difficulties have been overcome by the use of a mini-extrapolation chamber and radiochromic films.

The importance of establishing a reliable dosimetric procedure for the dermatologic applicators as done here is highlighted considering the fact that few applicators in Brazil are regularly recalibrated and their applications are based exclusively on the user manual information. The calculation methodology employed here reproduced well the experimental data and it has shown good agreement with the PDD curves reported in the protocol, so that, it can be utilized as an auxiliary guide for dosimetric characterization of similar dermatologic applicators.

Acknowledgments

The authors thank Dr. Mario Jefferson Quirino Louzada from the Biophysics Department of UNESP of Araçatuba-SP for the help in handling the radiochromic films and the Conselho Nacional de Desenvolvimento Científico e Tecnológico, CNPq, for funding part of this project.

References

[1] B. Guix, et al., Int. J. Radiat. Oncol. Biol. Phys. 50 (1) (2001) 167.
[2] M. Maarouf, et al., Strahlenther. Onkol. 177 (6) (2001) 330.
[3] H.B. Kal, R.E. Veen, Strahlenther. Onkol. 181 (11) (2005) 717.
[4] B.O. Junior, Medicina Faculty UNESP, 2007.
[5] S. Fukushima, T. Inoue, T. Inoue, S. Ozeki., Int. J. Radiat. Oncol. Biol. Phys. 43 (3) (1999) 597.
[6] I.M. Jürgenliemk-Schulz, et al., Int. J. Radiat. Oncol. Biol. Phys. 59 (4) (2004) 1138.
[7] T.Y. Eng, et al., Hematol./Oncol. Clin. North Am. 20 (2) (2006) 523.
[8] X-5 Monte Carlo Team, MCNP: A General Monte Carlo N-particle Transport Code, version 5, report LA-CP-03-0245 (Los Alamos National Laboratory), 2003.
[9] International specialty products, Gafchromic® EBT Self-Developing Film for Radiotheraphy Dosimetric, 〈http://online1.ispcorp.com/Gafchromic/content/products/ebt/pdfs/EBTwhitepaper.pdf〉.
[10] H.G. Hughes, Treating electron transport in MCNP report LA-UR-96-4583, Los Alamos National Laboratory, 1996.
[11] C. Moller, Ann. Physik. 14 (1932) 568.
[12] Netherlands Commission on Radiation Dosimetry, Report 14, Netherlands, 2004.
[13] ICRU 2004 Dosimetry of beta-rays and low-energy photons for brachytherapy with sealed sources ICRU report 72 (Bethesda, MD: International Commission on Radiation Units and Measurements).
[14] T.A. Ferreira, W. Rasband, The ImageJ User Guide version 1.43, 〈http://rsbweb.nih.gov/ij/docs/user-guide.pdf〉.